Journal of
Dental Research

Nano hydroxyapatite coated implants improves the bone nanomechanical properties

Journal:	*Journal of Dental Research*
Manuscript ID:	JDR-12-0553.R2
Manuscript Type:	Research Reports
Date Submitted by the Author:	25-Aug-2012
Complete List of Authors:	Jimbo, Ryo Coelho, Paulo; New York University, Biomaterials and Biomimetics Bryington, Matthew Baldassarri, Marta; NYU College of Dentistry, Biomaterials and Biomimetics Tovar, Nick; NYUCD, Biomaterials and Biomimetics Currie, Fredrik Hayashi, Mariko Andersson, Martin; Chemical and Biological Engineering Ono, Daisuke Vndeweghe, Stefan Wennerberg, Ann; Malmoe University, Dept. of Prosthetic Dentistry
Keywords:	Dental implant(s), Nanoindentation, Nanotechnology
Abstract:	Nanostructure modification of dental implants has long been sought as a mean to improve osseointegration through enhanced biomimicry of host structures. Several methods have been proposed and demonstrated for creating nanotopographic features; here we described a nanoscale hydroxyapatite (HA) coated implant surface and hypothesized that it will hasten osseointegration and improve its quality relative to non-coated implants. Twenty threaded titanium alloy implants, half prepared with stable HA nanoparticle surface and half grit-blasted, acid-etched, and heat treated (HT), were inserted into rabbit femurs. Preoperatively, the implants were morphologically and topographically characterized. After 3 weeks of healing, the samples were retrieved for histomorphometry. Moreover, the nanomechanical properties of the surrounding bone were evaluated using nanoindentation. While both implants revealed similar bone-to-implant contact, the nanoindentation demonstrated that the tissue quality was significantly enhanced around the HA-coated implants, validating the postulated hypothesis.

Date submitted: 6/20/2012

Date last revised: 8/25/2012

Date accepted: 9/11/2012

Nano hydroxyapatite coated implants improves bone nanomechanical properties

Ryo Jimbo[1], Paulo G Coelho[2], Matthew Bryington[3], Marta Baldassarri[2], Nick Tovar[2], Frederik Currie[4], Mariko Hayashi[1], Martin Andersson[5], Daisuke Ono[6], Stefan Vandeweghe[1,7], Ann Wennerberg[1]

1. Department of Prosthodontics, Faculty of Odontology, Malmö University, Sweden
2. Department of Biomaterials and Biomimetics, New York University, New York, USA
3. Division of Restorative and Prosthetic Dentistry, The Ohio State University College of Dentistry, Columbus, Ohio, USA
4. Promimic AB, Gothenburg, Sweden
5. Department of Chemical and Biological Engineering, Applied Surface Chemistry, Chalmers University of Technology, Gothenburg, Sweden
6. Division of Applied Prosthodontics, Nagasaki University Grraduate School of Biomedical Sciences, Nagasaki, Japan
7. Department of Periodontology and Oral Implantology, Dental School, Faculty of Medicine and Health sciences, University of Ghent, Belgium

Correspondence to; Ryo Jimbo, Department of Prosthodontics, Faculty of Odontology, Malmö University, 205 06 Malmö, Sweden

Fax + 46 40 665 8503

Phone +46 40 665 8679

E-mail: ryo.jimbo@mah.se

Running title: Nanomechanical evaluation of nano HA implants

Word counts: 2,694

Number of figures: 4

Abstract counts: 138

ABSTRACT

Nanostructure modification of dental implants has long been sought as a mean to improve osseointegration through enhanced biomimicry of host structures. Several methods have been proposed and demonstrated for creating nanotopographic features; here we described a nanoscale hydroxyapatite (HA) coated implant surface and hypothesized that it will hasten osseointegration and improve its quality relative to non-coated implants. Twenty threaded titanium alloy implants**,** half prepared with stable HA nanoparticle surface and half grit-blasted, acid-etched, and heat treated (HT), were inserted into rabbit femurs. Preoperatively, the implants were morphologically and topographically characterized. After 3 weeks of healing, the samples were retrieved for histomorphometry. Moreover, the nanomechanical properties of the surrounding bone were evaluated using nanoindentation. While both implants revealed similar bone-to-implant contact, the nanoindentation demonstrated that the tissue quality was significantly enhanced around the HA-coated implants, validating the postulated hypothesis.

Keywords: osseointegration; nano-hydroxyapatite coating; nanoindenter; histomorphometry

INTRODUCTION

The current trend for biomaterial modification has a specific direction, to enhance the bioactivity to functionally, structurally, and in principle, replace the native organ. Throughout the history of biomedical engineering, we have learned that mimicking from biology would be the ultimate modification, and hierarchical biomimetic architecture leads to the creation of different functional elements (Alberts et al., 2002). Nanoscale alterations has been suggested to increase its bioactivity (Goransson et al., 2009), and is now evident that various molecular interactions occur at this size level (Dalby et al., 2002).

Nanostructures applied to biomaterials have been suggested to contribute to higher grade of osseointegration (Ellingsen et al., 2004), and it has been shown that biology responds sensitively to different nanostructures (Coelho et al., 2011; Jimbo et al., 2012). In fact, Webster and Ahn specified that nanostructures below 100 nm in size are most effective in cellular integration and suggested that these should be differentiated from the so-called submicron structures (Webster and Ahn, 2007). What is unique about the effect of HA nanocoating is that the stimulatory outcomes are related not only to the topography, but also to the effect of chemistry, which generates a synergetic effect (Jimbo et al., 2012). Further, compared to the traditional 'thick' HA coatings, which generated clinical problems (Albrektsson, 1998), the mono-layered thin HA-coating seems to be stable and shows no signs of foreign body reaction (Jimbo et al., 2012).

In a previous study observing the gene expression around turned-nano HA-coated implants, the nano HA-coating significantly enhanced osteogenic gene expression while increasing osteoclastic activity suggesting the nano HA is actively involved in the bone formation (Jimbo et al., 2011b).

However, some studies have shown that the biological outcomes of the same coating do not present enhancing results (Svanborg et al., 2011) due to several factors. Therefore, three-dimensional evaluation using the micro computed tomography has been implemented in order to compensate and to obtain further detailed information (Jimbo et al., 2011a). In this study, the effect of nanostructured HA-coating was evaluated histologically. Further in order to determine the nanomechanical properties of the surrounding bone around the implant, a nanoindentation testing was conducted based on the hypothesis that the mechanical aspect of the bone is improved due to the effect of the nanostructured HA.

MATERIALS & METHODS

Implant Surface Preparation

Twenty threaded implants (Ti6Al4V, Ø3.3 × 6 mm) were used. All implants were sandblasted and acid etched (Aadva surface, GC Dental, Tokyo Japan). Half of the implants (HA) were coated with nano-sized HA according to the Promimic HA^{nano}™ method (Jimbo et al., 2012). The other half of the implants were subjected to only heat treatment in the same manner as the HA implants (HT).

Morphological characterization

Surface morphology of the randomly selected implants from each group was examined by scanning electron microscopy (SEM, LEO Ultra 55 FEG, Zeiss,

Oberkochen, Germany) at an accelerating voltage of 6 kV (n=3).

In order to confirm that the microtopography had not changed by the nano HA coating, surface topography was characterized by an optical interferometer (MicroXam; ADE Phase Shift, Inc., Tucson, AZ, USA). Three implants from each group were randomly selected and each of them measured on 9 regions (3 tops, 3 thread valleys, and 3 flanks).

The parametric calculation was performed after the removal of errors of form and waviness by the use of a Gaussian filter (50 × 50 μm).

Implantation and sample preparation

The animal study was approved by the Malmö/Lund, Sweden, regional animal ethics committee (approval number: M282-09). One HA and one HT implant were inserted into the left and right tibia, respectively, of 10 adult Swedish lop-eared rabbits (mean weight, 4.2 kg). The animals were anesthetized with intramuscular injections of a mixture of 0.15 mL/kg medetomidine (1 mg/mL Dormitor; Orion Pharma, Sollentuna, Sweden) and 0.35 mL/kg ketamine hydrochloride (50 mg/mL Ketalar; Pfizer AB, Sollentuna, Sweden). Lidocaine hydrochloride (Xylocaine; AstraZeneca AB, Södertälje, Sweden) was administered as local anesthetic at each insertion site at a dose of 1 mL. After the surgical site exposure, osteotomy was prepared using a series of drills (final diameter Ø2.9), and thereafter, the implants were inserted. Post-operatively, buprenorphine hydrochloride (0.5 mL Temgesic; Reckitt Benckiser, Slough, UK) was administered as an analgesic for 3 days. In order to observe the early bone formation and to compare the outcomes of the study to other studies using the nano HA-coated surface (Svanborg et al., 2011), a time point of 3 weeks was chosen.

At 3 weeks postoperatively, the rabbits were euthanized and the bone samples were retrieved and placed in 4% formaldehyde for 24 h; thereafter, were placed in a series of dehydration and infiltration baths, and finally, were embedded in light-curing resin (Technovit 7200 VLC; Heraeus Kulzer Wehrheim, Germany).

Ground sectioning and histological analysis

All samples were processed for undecalcified ground sectioning. In brief, the embedded samples were cut in the middle of the implant, and one central undecalcified cut and ground section of approximately 15 µm was prepared and stained with toluidine blue and pyronin G. Histological evaluation was performed using a light microscope (Eclipse ME600; Nikon, Japan), and histomorphometrical data were analyzed by Image J (v. 1.43u; National Institutes of Health). The bone-to-implant contact (BIC) along the entire implant was calculated at ×10 to ×40 objective magnification.

Nanoindentation

The remaining resin blocks were processed in the same manner as the histological sections (thickness: approximately 100µm); further polishing was performed to remove scratches using diamond suspensions of 9 to 1 µm particle size (Buehler, Lake bluff, IL, USA). Nanoindentation (n=28/specimen) was performed using a nanoindenter (Hysitron TI 950, Minneapolis, MN, USA) equipped with a Berkovich diamond three-sided pyramid probe (Baldassarri et al., 2012). A wax chamber was created so that tests were performed in distilled water (Wallace, JM, 2012). A loading profile was developed using a peak load of 300 µN at a rate of 60 µN/s, followed by a holding time of 10 s and an unloading time of 2 s as presented in

Figure 1B. The extended holding period allowed bone to relax to a more linear response, so that no tissue creep effect was occurring in the unloading portion of the profile (ISO 14577-4). Therefore, from each indentation a load-displacement curve was obtained, presented in Figure 1B (Oliver and Pharr, 1992a).

For each specimen, mechanical testing was performed in the threaded region (cortical area), in which generally new bone formation is present at early observation time points. Since interfacial bone modeling and remodeling (and potentially bone kinetics and mechanical properties) has been shown to change as a function of the interplay between surgical instrumentation and implant geometry (Coelho et al., 2010), the region between threads was subdivided into four bone quadrants as depicted in Figure 1C. Bone tissue was detected by imaging under the light microscope (Hysitron TI 950, Minneapolis, MN, USA)(Butz et al., 2006) and indentations were performed in the selected areas. From each analyzed load-displacement curve, reduced modulus (GPa) and hardness (GPa) of bone tissue were computed and its elastic modulus Eb (GPa) was calculated as follows:

$$\frac{1}{E_r} = \frac{1-\nu^2}{E} + \frac{1-\nu_i^2}{E_i}$$

where Er is the reduced modulus (GPa), ν (0.3) is the Poisson's ratio for cortical bone, Ei (1140 GPa) and νi (0.07) are the elastic modulus and Poisson's ratio for the indenter (Hoffler et al., 2000; Hoffler et al., 2005; Oliver and Pharr, 1992b).

Statistical Analysis

The mean values of surface roughness were compared by one-way ANOVA, followed by a post hoc Tukey–Kramer test with the significant level set at 0.05. The

non-parametric Wilcoxon signed-rank test was used for bilaterally inserted implants with the significance level set at 0.05. For the nanomechanical testing, linear mixed models were performed in order to determine the influence of different surfaces (HA vs HT) and bone position within threads (Figure 1C) on rank elastic modulus and rank hardness values (statistical summaries for the different variables are also presented but statistical inferences were made based on ranked data).

RESULTS

Morphologic and topographic analysis

SEM micrographs of both groups are presented in Figure 2A-D. At high magnification, it is evident that the HA-coated surface was fully covered with rod-shaped HA particles approximately 10–15 nm wide and 100–200 nm in length (Figure 2D).

No significant topographical differences between the two groups in the micro level were seen, thus, it was confirmed that the microtopography was not altered by the nano HA coating (Figure 2E).

Histomorphometry

The histological sections presented newly formed trabeculae with deeply stained mineralized tissue for both groups after 3 weeks of healing, and no visible differences in bone formation could be confirmed, as presented in Figure 3A.

The mean BIC (SD) values for the HT and HA groups are presented in Figure 3B. In brief, the BIC for the entire threads were 32.1% (9.9) and 35.7% (8.0) for the HT and HA groups, respectively. There were no significant differences between the two groups. ($p = 0.21$).

Nanoindentation

The mean ± SE elastic modulus and hardness for the HA group was 6.01± 0.40 GPa and 0.29 ± 0.025 GPa, respectively. For the HT group, the mean ± SE elastic modulus and hardness were 2.69 ± 0.19 GPa and 0.14 ± 0.007 GPa, respectively (Figure 4A). Significantly higher levels of hardness rank and elastic modulus rank were observed for the HA group relative to the HT group (H= $p<0.001$; E= $p<0.001$, Figures 4B and 4D). No significant differences in the levels of both hardness rank and elastic modulus rank were observed between positions 1-4 (H= $p=0.17$; E= $p=0.18$, Figures 4B and 4D). When surface group and position were evaluated altogether, significantly higher values of hardness rank and elastic modulus rank were observed for the HA group relative to the HT group at all positions (Figures 4C and 4E).

DISCUSSION

The method to determine the degree of osseointegration was mainly dependent on histology/histomorphometry and biomechanics. However, it has been discussed that these evaluation techniques may not actually capture the entire phenomenon. Especially when evaluating the effect of nanometer structures, detailed evaluation approaches are essential to clarify their roles during osteogenesis (Jimbo et al., 2011a; Jimbo et al., 2011b). In our previous study, we reported that the presence of HA nanotopography on implant surfaces enhanced osteogenic markers such as alkaline phosphatase and osteocalcin and at the same time suppresses inflammation. It is strongly suggested that the chemico-topographical modification in the nano-level

enhances the bioactivity and osteogenesis, which was difficult to prove with conventional methodologies.

The histomorphometric results of the current study did not show statistical differences between the test and the control surfaces. Both surfaces presented high BIC after 3 weeks, which is a commonly selected time point in a rabbit model to evaluate early bone response (Svanborg et al., 2011). These enhanced histomorphometric outcomes seen for both surfaces may be attributed to the base surface topography, which had a moderately rough micro topography (Wennerberg and Albrektsson, 2009). The significant impact of the sandblasting, and acid etching may have hindered the effect of the nanostructures, at least in the morphometric evaluation. Further, since the coating layer is a monolayer of less than 100 nm and it is known to metabolize into the living system, remnants of HA particles could not be observed microscopically and no inflammatory responses were detected, as it was the case with thicker HA coatings (Albrektsson, 1998; Reigstad et al., 2011). Thus, qualitatively and quantitatively from a morphologic evaluation, no differences could be detected.

Intriguingly, bone nanomechanical testing showed that the tissue properties were uniform throughout the evaluated (all four quadrants) region for each group by significantly enhanced for the HA group relative to the control. Both the rank elastic modulus and rank hardness presented significantly higher values regardless of different regions, suggesting that the presence of nano HA had an effect both at the immediate interfacial regions and the relatively distant regions. It has been reported that bone nanomechanical properties are strongly correlated to the intrinsic material property of the tissue, *i.e.*, mineralisation of the bone or characteristics of the organic matrix (Boivin et al., 2008; Currey, 1975). More specifically, the calcium content of

bone and the Young's modulus have been suggested to have a positive relationship (Currey, 1988). It is a fact that the properties of the collagen fibers will be affected by formalin fixation, thus and properties through nanoindentation, while in larger scale than collagen fiber level, could be affected. However, since both groups were subjected to the exact same fixation process, it is most likely that the two groups examined in this study were compared on a relative basis and possibly not by an absolute bone mechanical property basis.

A possible explanation for the higher mineralization could be that the calcium and the phosphate released from the surface had been incorporated to the surrounding new bone, therefore, strengthening the mineralization properties. Although in general, it has been known that hydroxyapatites are the most stable form of the calcium phosphate family, the apatite nanoparticles that has been utilized in this study was synthesized according to a soft-templating method (He et al., 2012). According to this method, the apatite formed has a high resemblance to the apatite found in bone, with a small particle size, relatively low crystallinity, calcium deficiency and carbonated. Thus, the nano HA used in this study is a soluble form of hydroxyapatite. This phenomenon has been confirmed by Wennerberg *et al.* (2011), who found that radio labelled 45Ca coated to the implant gradually detached from its surface and was localized in the surrounding new bone, which eventually was metabolized (Wennerberg et al., 2011).

Another possible explanation is the effect of nanostructures enhancing the mineralization. As suggested by Tsukimura et al., nanostructured surfaces enhanced the mineralization of rat bone marrow-derived osteoblasts (Tsukimura et al., 2011). It

is suggested that along with the effect of chemistry, the effect of topography was involved in the enhancement.

Furthermore, the highly active mineralization cascade of the interfacial bone around the nanostructured HA-coated implants can be explained from a genetic aspect. It has been reported that alkaline phosphatase expression in bone around nanostructured HA-coated implants was significantly higher than that of the bone around the non-coated surfaces, and the relative expression differences between the HT and HA surfaces amplified over time (Jimbo et al., 2011b). Since high alkaline phosphatase activity enhances osteopontin expression, which is known to be a cohesive factor for mineralization, it is suggested that HA-coating was partly responsible for the enhanced bone nanomechanical properties.

Although osseointegration is defined from direct measurement of bone-to-implant contact, the clinical interest today is focusing more on the stability of the implant that will withstand dynamic loading. Needless to say, this would require new bone formation, at the same time; the mineralization level of forming bone may be an essential factor. Using the nanoindenter, capabilities of the nano HA to strengthen the bone quality are evidenced, validating the hypothesis that nanoscale HA-coated implant surface will hasten the quality of osseointegration.

While initial bone apposition is an important aspect of osseointegration, longer healing periods especially those experiencing dynamic loading are of greater clinical interest. This study thus presents purely experimental findings as only a single 3 week observation was made. Further studies are required to develop conclusions of clinical performance.

ACKNOWLEDGEMENTS

GC Dental is acknowledged for providing the implants. This study was funded by the grants from the Swedish Knowledge Foundation. The authors declare no conflict of interests.

REFERENCES

Alberts B, Johnson A, Lewis J, Raff M, Roberts K, Walter P (2002). Molecular Biology of the Cell. New York, NY: Garland Science.

Albrektsson T (1998). Hydroxyapatite-coated implants: a case against their use. *J Oral Maxillofac Surg* 56:1312-1326.

Albrektsson T, Wennerberg A (2004). Oral implant surfaces: Part 1--review focusing on topographic and chemical properties of different surfaces and in vivo responses to them. *Int J Prosthodont* 17:536-543.

Baldassarri M, Bonfante E, Suzuki M, Marin C, Granato R, Tovar N, *et al.* (2012). Mechanical properties of human bone surrounding plateau root form implants retrieved after 0.3-24 years of function. *J Biomed Mater Res B Appl Biomater* 100B:2015-2021.

Bhushan B (2009). Biomimetics: lessons from nature--an overview. *Philos Transact A Math Phys Eng Sci* 367:1445-1486.

Boivin G, Bala Y, Doublier A, Farlay D, Ste-Marie LG, Meunier PJ, *et al.* (2008). The role of mineralization and organic matrix in the microhardness of bone tissue from controls and osteoporotic patients. *Bone* 43:532-538.

Butz F, Aita H, Wang CJ, Ogawa T (2006). Harder and stiffer bone osseointegrated to roughened titanium. *J Dent Res* 85:560-565.

Coelho PG, Suzuki M, Guimaraes MV, Marin C, Granato R, Gil JN, *et al.* (2010). Early bone healing around different implant bulk designs and surgical techniques: A study in dogs. *Clin Implant Dent Relat Res* 12:202-208.

Coelho PG, Freire JN, Granato R, Marin C, Bonfante EA, Gil JN, *et al.* (2011). Bone mineral apposition rates at early implantation times around differently prepared titanium surfaces: a study in beagle dogs. *Int J Oral Maxillofac Implants* 26:63-69.

Currey JD (1975). The effects of strain rate, reconstruction and mineral content on some mechanical properties of bovine bone. *J Biomech* 8:81-86.

Currey JD (1988). The effect of porosity and mineral content on the Young's modulus of elasticity of compact bone. *J Biomech* 21:131-139.

Dalby MJ, Riehle MO, Johnstone HJ, Affrossman S, Curtis AS (2002). Polymer-demixed nanotopography: control of fibroblast spreading and proliferation. *Tissue Eng* 8*:*1099-1108.

Ellingsen JE, Johansson CB, Wennerberg A, Holmen A (2004). Improved retention and bone-tolmplant contact with fluoride-modified titanium implants. *Int J Oral Maxillofac Implants* 19*:*659-666.

Goransson A, Arvidsson A, Currie F, Franke-Stenport V, Kjellin P, Mustafa K, *et al.* (2009). An in vitro comparison of possibly bioactive titanium implant surfaces. *J Biomed Mater Res A* 88*:*1037-1047.

He W, Kjellin P, Currie F, Handa P, Knee CS, Bielecki J, *et al.* (2011). Formation of Bone-like Nanocrystalline Apatite Using Self-Assembled Liquid Crystals. *Chemistry of Materials* 24*:*892-902.

Hoffler CE, Moore KE, Kozloff K, Zysset PK, Brown MB, Goldstein SA (2000). Heterogeneity of bone lamellar-level elastic moduli. *Bone* 26*:*603-609.

Hoffler CE, Guo XE, Zysset PK, Goldstein SA (2005). An application of nanoindentation technique to measure bone tissue Lamellae properties. *J Biomech Eng* 127*:*1046-1053.

Jimbo R, Coelho PG, Vandeweghe S, Schwartz-Filho HO, Hayashi M, Ono D, *et al.* (2011a). Histological and three-dimensional evaluation of osseointegration to nanostructured calcium phosphate-coated implants. *Acta Biomater* 7*:*4229-4234.

Jimbo R, Xue Y, Hayashi M, Schwartz-Filho HO, Andersson M, Mustafa K *et al.* (2011b). Genetic responses to nanostructured calcium-phosphate-coated implants. *J Dent Res* 90*:*1422-1427.

Jimbo R, Sotres J, Johansson C, Breding K, Currie F, Wennerberg A (2012). The biological response to three different nanostructures applied on smooth implant surfaces. *Clin Oral Implants Res* 23*:*706-712.

Oliver WC, Pharr GM (1986). A method for interpreting the data from depth-sensing indentation instruments. J Mater Res 1:601-609.

Oliver WC, Pharr GM (1992). An Improved Technique for Determining Hardness and Elastic-Modulus Using Load and Displacement Sensing Indentation Experiments. *J Mater Res* 7*:*1564-1583.

Puckett SD, Taylor E, Raimondo T, Webster TJ (2010). The relationship between the nanostructure of titanium surfaces and bacterial attachment. *Biomaterials* 31*:*706-713.

Reigstad O, Johansson C, Stenport V, Wennerberg A, Reigstad A, Rokkum M (2011). Different patterns of bone fixation with hydroxyapatite and resorbable CaP coatings in the rabbit tibia at 6, 12, and 52 weeks. *J Biomed Mater Res B Appl Biomater* 99*:*14-20.

Seeman E, Delmas PD (2006). Bone quality--the material and structural basis of bone strength and fragility. *N Engl J Med* 354*:*2250-2261.

Svanborg LM, Hoffman M, Andersson M, Currie F, Kjellin P, Wennerberg A (2011). The effect of hydroxyapatite nanocrystals on early bone formation surrounding dental implants. *Int J Oral Maxillofac Surg* 40*:*308-315.

Tsukimura N, Yamada M, Iwasa F, Minamikawa H, Att W, Ueno T *et al.* (2011). Synergistic effects of UV photofunctionalization and micro-nano hybrid topography on the biological properties of titanium. *Biomaterials* 32*:*4358-4368.

Webster TJ, Ahn ES (2007). Nanostructured biomaterials for tissue engineering bone. *Adv Biochem Eng Biotechnol* 103:275-308.

Wennerberg A, Albrektsson T (2009). Effects of titanium surface topography on bone integration: a systematic review. *Clin Oral Implants Res* 20(Suppl 4):172-184.

Wennerberg A, Jimbo R, Allard S, Skarnemark G, Andersson M (2011). In vivo stability of hydroxyapatite nanoparticles coated on titanium implant surfaces. *Int J Oral Maxillofac Implants* 26*:*1161-1166.

FIGURE LEGENDS

Figure 1: (A) Drill sequence used for the implantation. (B) Load in vivo time quasi-static testing profile, and a representative load displacement graph of the nanoindentation analysis. (C) The region of interest created for the study. The area within the thread of was subdivided into four quadrants in order to determine whether there is a area differences in the bone nanomechanical properties.

Figure 2: Surface morphologic properties investigated by scanning electron microscopy. Lower magnification images for (A) heat treated (HT), and (B) nano hydroxyapatite-coated (HA) implant surface. At this magnification (error bars: 1 μm), the rough surface structure of the base substrate can be seen and is difficult to see detailed differences between the two groups. The higher magnification images (marker bars: 200 nm) clearly indicate differences between the (C) HT, and the (D) HA surface. It is evident that the needle-like structure of about 100 nm in length fully covers the surface for the HA surface. (E) Surface topography measurements conducted by the optical interferometer. No statistical differences were detected in the micro-level.

Figure 3: Descriptive histologic images of the HT and HA implants placed in the rabbit tibia. For both groups, it was evident that new bone formed from the existing bone, and was in contact to the implant surface. No differences were noted between the two groups.

Figure 4: (A) Graph representing the mean hardness (GPa) and elastic modulus (GPa) for the HA and HT groups. (B) Summary statistics (rank of each property ± 95% confidence interval) for rank hardness as a function of implant surface group and rank hardness as a function of different positions (1-4). (C) Rank hardness as a function of implant surface group and different positions (1-4). (D) Summary statistics (rank of each property ± 95% confidence interval) for rank modulus as a

function of implant surface group and rank modulus as a function of different positions (1-4). (E) Rank modulus as a function of implant surface group and different positions (1-4).

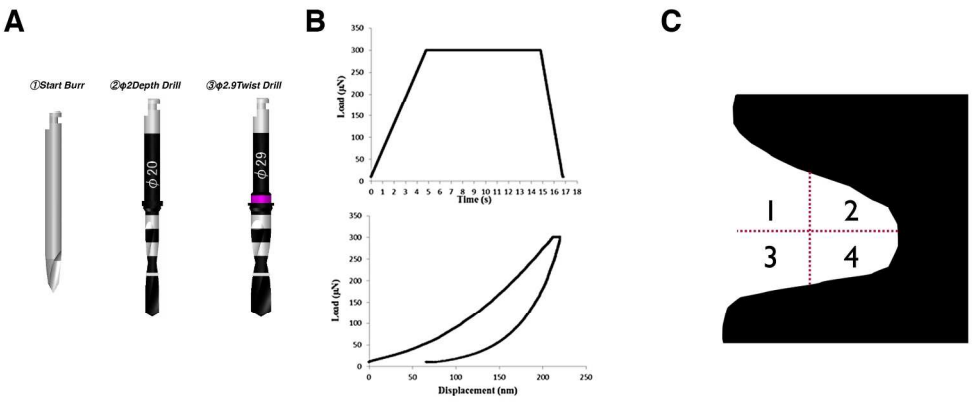

(A) Drill sequence used for the implantation. (B) Load in vivo time quasi-static testing profile, and a representative load displacement graph of the nanoindentation analysis. (C) The region of interest created for the study. The area within the thread of was subdivided into four quadrants in order to determine whether there is a area differences in the bone nanomechanical properties.
211x89mm (300 x 300 DPI)

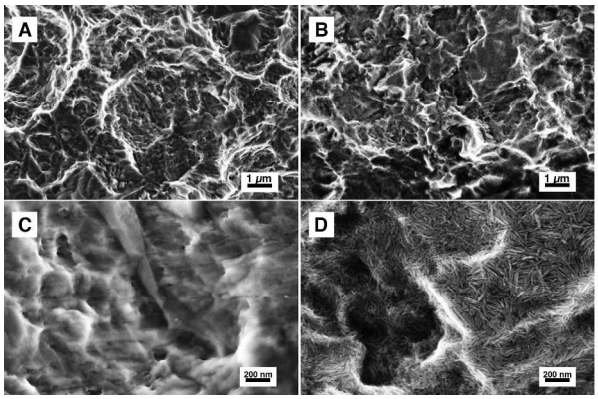

E

Groups	$S_a \pm SD$ (µm)	$S_{dr} \pm SD$ (%)	$S_{ds} \pm SD$ (per mm^2)
HT	1.03±0.14	30.25±5.86	134,868±7094
HA	0.94±0.12	27.44±1.54	139,359±9367

Surface morphologic properties investigated by scanning electron microscopy. Lower magnification images for (A) heat treated (HT), and (B) nano hydroxyapatite-coated (HA) implant surface. At this magnification (error bars: 1 µm), the rough surface structure of the base substrate can be seen and is difficult to see detailed differences between the two groups. The higher magnification images (marker bars: 200 nm) clearly indicate differences between the (C) HT, and the (D) HA surface. It is evident that the needle-like structure of about 100 nm in length fully covers the surface for the HA surface. (E) Surface topography measurements conducted by the optical interferometer. No statistical differences were detected in the micro-level.
254x98mm (300 x 300 DPI)

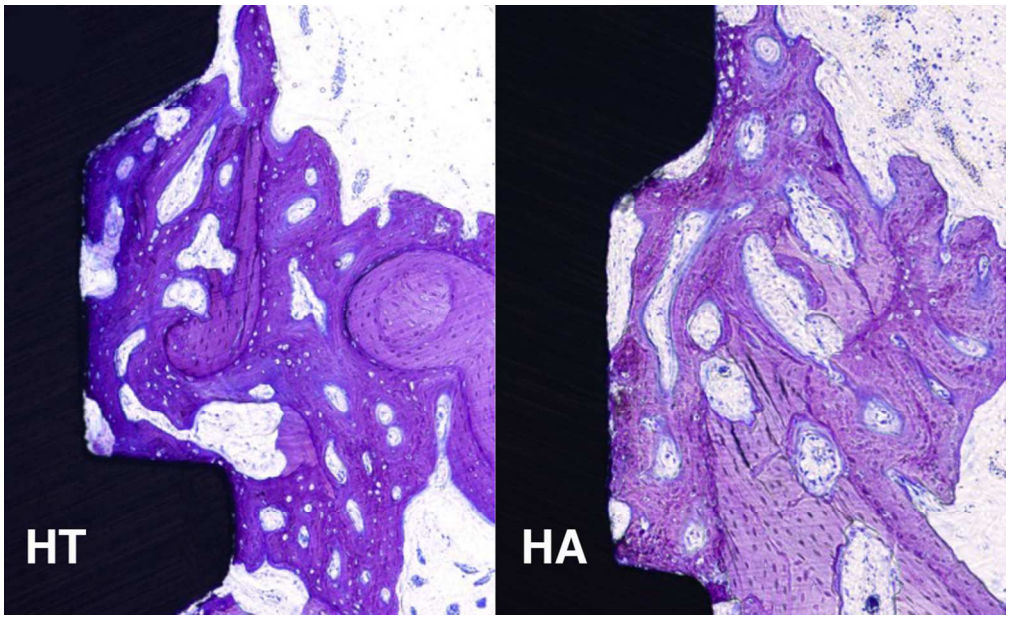

Descriptive histologic images of the HT and HA implants placed in the rabbit tibia. For both groups, it was evident that new bone formed from the existing bone, and was in contact to the implant surface. No differences were noted between the two groups.
106x64mm (300 x 300 DPI)

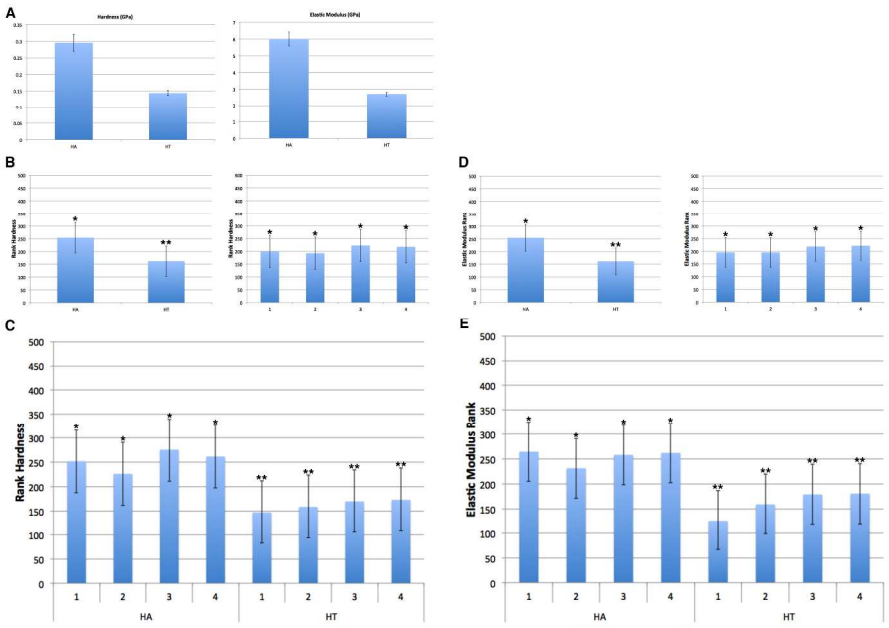

(A) Graph representing the mean hardness (GPa) and elastic modulus (GPa) for the HA and HT groups. (B) Summary statistics (rank of each property ± 95% confidence interval) for rank hardness as a function of implant surface group and rank hardness as a function of different positions (1-4). (C) Rank hardness as a function of implant surface group and different positions (1-4). (D) Summary statistics (rank of each property ± 95% confidence interval) for rank modulus as a function of implant surface group and rank modulus as a function of different positions (1-4). (E) Rank modulus as a function of implant surface group and different positions (1-4).
338x213mm (300 x 300 DPI)